Oscillatory and pulsatile flows in environmental, biological and industrial applications

Rafik Absi

▶ **To cite this version:**

Rafik Absi. Oscillatory and pulsatile flows in environmental, biological and industrial applications. 8th International Conference on Fluid Mechanics (ICFM8), Sep 2018, Tohoku, Japan. ⟨hal-02358715⟩

HAL Id: hal-02358715

https://hal.science/hal-02358715v1

Submitted on 12 Nov 2019

HAL is a multi-disciplinary open access archive for the deposit and dissemination of scientific research documents, whether they are published or not. The documents may come from teaching and research institutions in France or abroad, or from public or private research centers.

L'archive ouverte pluridisciplinaire **HAL**, est destinée au dépôt et à la diffusion de documents scientifiques de niveau recherche, publiés ou non, émanant des établissements d'enseignement et de recherche français ou étrangers, des laboratoires publics ou privés.

HAL Authorization

Proceedings of the 8th International Conference on Fluid Mechanics (ICFM8)
September 25-28, 2018, Tohoku University, Sendai, Japan

Oscillatory and pulsatile flows in environmental, biological and industrial applications

Rafik Absi [1,2,*]

[1] *EBI, 49 avenue des Genottes, CS 90009, 95895 CERGY Cedex, FRANCE*
[2] *ECAM-EPMI, Inst. Polytech. St-Louis, 13 Boulevard de l'Hautil, 95000 CERGY, FRANCE*

Abstract: The understanding of oscillatory and pulsatile flows is of high interest for different environmental/coastal, biological/health and industrial applications. Marine and coastal environment is dominated by waves. The related oscillatory turbulent boundary layers are involved in different coastal engineering applications. In the circulatory system, the study of the pulsatile flow of blood is indispensable for the better comprehension of many cardiovascular diseases. In bio-industries, pulsed flows are used in the cleaning of fouling deposits in different equipment. These different flows require deep understanding of advanced concepts in fluid mechanics and need an adequate quantification of the involved parameters such as wall shear stress (WSS). This study shows interdisciplinary knowledge from different communities: Environment/Coastal engineering, Health/Medicine and Bio-Industries/Chemical engineering. The knowledge acquired within a specialty could be of interest to others. It is important to share and use knowledge beyond disciplines especially in fluid mechanics which is at the crossroads of different applications. This study aims transdisciplinary research strategies toward a holistic approach.

Key words: Oscillatory flow, pulsating flow, wall shear stress (WSS), waves, arteries, fouling deposits

1. Introduction

Over these last decades, research in fluid mechanics has shown a real enthusiasm for the understanding of periodic (oscillatory and pulsatile) flows. This was motivated by potential applications in the environmental/coastal, biological/health and bio-industrial sectors.

Marine and coastal environment is dominated by waves. This motion produces an oscillatory flow near the bottom (Jonsson, 1966). The understanding of these flows required many theoretical, experimental and numerical studies (Kajiura, 1968). In addition to wave flume experiments, oscillating water tunnel measurements were of crucial importance to better understand oscillatory turbulent boundary layers (Jensen *et al.*, 1989). This knowledge is important for the study of coastal sediment transport (Fredsoe and Deigaard, 1992; Nielsen, 1992; van Rijn, 1993).

The flow of blood is pulsatile in the circulatory system. Its study is indispensable to understand better many cardiovascular diseases (Rammos *et al.*, 1998). Physiological and cardiovascular fluid mechanics provide an understanding of advanced concepts in fluid mechanics related to pulsatile flows in elastic tubes as arteries (Canic, 2002, Mynard, 2010).

Pulsed flows are used in the cleaning of fouling deposits in bio-industrial equipment (Gillham *et al.*, 2000; Blel *et al.*, 2009). Cleaning needs to be more optimized by reducing excess energy and excessive resources (water and chemicals). This optimization needs an adequate quantification of the involved parameters such as forces/energy required for the removal of deposits.

Wall shear stress (WSS) is a parameter of common interest. In coastal engineering, it is involved in the incipient motion of sediments and in turbulence modeling. In medicine, WSS is related to several endothelial dysfunction and cardiovascular disease as atherosclerosis. In industry, deposit removal depends on WSS values.

The principles of conservation of mass, momentum and energy provide the main equations of fluid flow which are non-linear, partial differential equations and need numerical solutions. Computational fluid dynamics (CFD) modelling provides detailed pressure and flow fields and the quantification of the involved parameters. For some cases, it is possible to obtain analytical solutions from simplifications of these equations (Absi, 2008).

* Corresponding author. Email: r.absi@hubebi.com ; rafik.absi@yahoo.fr

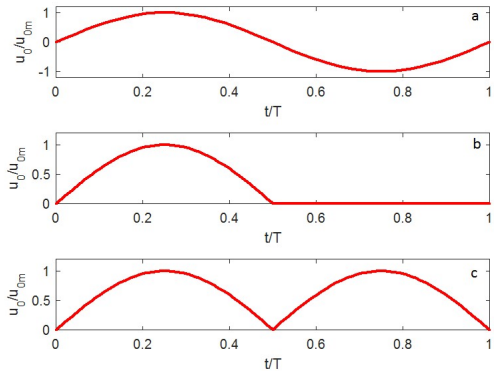

Figure 1. Pure oscillatory flow (a) and simple pulsating flows (b) and (c).

Figure (1) shows simple pulsed flows based on a pure oscillatory flow (fig. 1, a) given by the free stream velocity of the wave bottom boundary layer

$$u_0(t) = u_{0m}\sin(\omega\, t) \qquad (1)$$

Where $\omega = 2\pi/T$, T is the period. A simple pulsatile flow (fig. 1, b) given by

$$u_0(t) = \begin{cases} u_{0m}\sin(\omega\, t) & \text{if} \quad t \in [0, T/2] \\ 0 & \text{if} \quad t \in [T/2, T] \end{cases} \qquad (2)$$

which is a schematic representation of the systolic and diastolic phases of the cardiac cycle. Another simple pulsed flow (fig. 1, c) given by

$$u_0(t) = |u_{0m}\sin(\omega\, t)| \qquad (3)$$

has a shape similar to those used in cleaning of industrial equipment. These three flows are identical in the first half-period and therefore same methods could be applied there.

In the following sections, we will present first the results related to wave boundary layers, then to pulsatile flows in arteries and finally to pulsed flows for the cleaning of industrial equipment.

2. Oscillatory bottom boundary layers

The resolution of coastal engineering problems such as transport of sediments needs the understanding of the bottom boundary layer flow. The turbulent wave boundary layer has been the subject of many researchers: Kajiura (1968), Myrhaug (1982), Sleath (1990), Fredsoe and Deigaard (1992), Nielsen (1992), van Rijn (1993), Tanaka and Thu (1994) and others.

The distribution of eddy viscosity ν_t within the oscillatory boundary layer generated by waves is a key parameter in coastal engineering. Adequate description of eddy viscosity distribution in boundary layers is needed for accurate predictions of velocity profiles. Eddy viscosity is also related to sediment diffusivity which is involved in the calculation of sediment concentration profiles and therefore for the prediction of sediment transport by waves. For practical applications in coastal engineering, the eddy viscosity is obtained by RANS turbulence models as two-equation models (k-ε, k-ω, …), or by simple analytical formulations. The well-known are the parabolic-uniform profile (Myrhaug 1982, van Rijn 1993, Liu and Sato 2006) and the exponential-linear profile (Hsu and Jan 1998, Absi 2010). The *exponential-linear profile* is an exponential law modulated by a linear function given by

$$\nu_t = \alpha\, \kappa\, u_* z e^{(-C\, z/z_h)} \qquad (4)$$

where u_* is the friction velocity, z_h is the water depth or the distance from the wall to the axis of symmetry (for oscillatory water tunnel experiments) or free surface, $\kappa = 0.41$, α and C are coefficients. The validation and calibration of this analytical profile were performed by comparisons with the period-averaged eddy viscosity obtained from the BSL k-ω model (Menter, 1994; Suntoyo and Tanaka, 2009) for different wave conditions through the parameter a_m/k_s where a_m is the wave orbital amplitude and k_s is the equivalent roughness (Absi *et al.*, 2012).

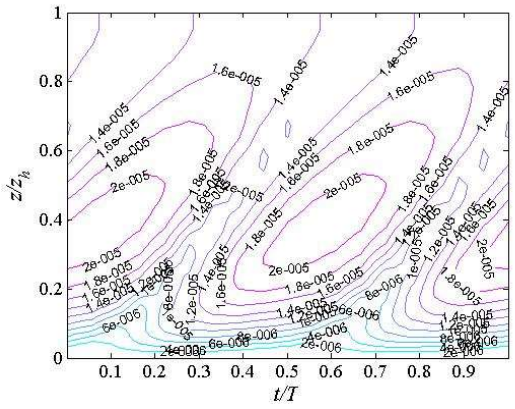

Figure 2. Temporal and Spatial Variation of dimensionless eddy viscosity for a sinusoidal wave obtained by the BSL k-ω model, Flow conditions: U0=3,63 m/s ; am=1,73 m ; T=3 s ; ks=1,5 cm, Re=437000.

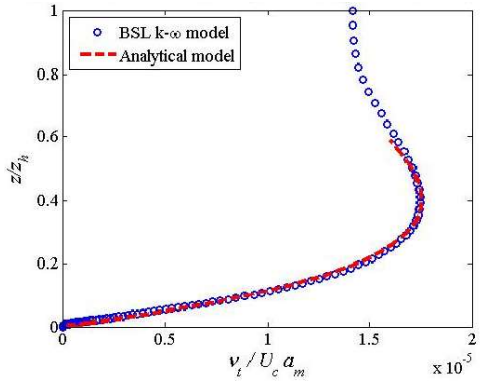

Figure 3. Period-averaged dimensionless eddy viscosity for a sinusoidal wave.

Figure (2) presents temporal and spatial variation of dimensionless eddy viscosity for a sinusoidal wave given by Eq. (1). Figure (3) shows comparison between period-averaged eddy viscosity obtained from the BSL k-ω model (symbols) and Eq. (4) (dashed line). Even if the eddy viscosity is highly time-dependent (fig. 2), the period-averaged dimensionless eddy viscosity has a shape which is well described by Eq. (4) for $z/z_h < 0.6$ (fig. 3). Figure (4) shows the comparison for an asymmetric wave given by

$$u(t) = u_1 \sin(\omega\, t) - u_2 \cos(2\, \omega\, t) \qquad (5)$$

Even for the case of asymmetric wave, the period-averaged dimensionless eddy viscosity has a shape which is well described by Eq. (4) for $z/z_h < 0.5$ (fig. 4). Figures (3) and (4) show that the period-averaged eddy viscosity profiles for sinusoidal and asymmetric waves are different. This indicates that the period-averaged eddy viscosity profile should depend on the wave non-linearity parameter given by $N_i=(u_1+u_2)/(2u_1)$ or $N_i=u_c/\hat{u}$, where u_c is the velocity at wave crest and $\hat{u}$ is the total velocity amplitude.

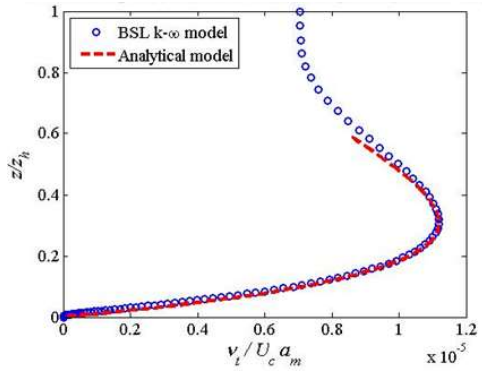

Figure 4. Period-averaged dimensionless eddy viscosity for asymmetric wave N_i=0.67.

Equation (4) needs the friction velocity which is related to wall shear stress (WSS). In coastal engineering, WSS could be obtained by simple methods as wave friction factor $f_w = \tau_w / \left(\frac{1}{2}\, \rho\, u_0^2\right)$ (Jonsson, 1966) or the momentum integral method (Fredsoe and Deigaard, 1992).

In the case of uniform flow, the momentum equation is

$$\rho \frac{\partial u}{\partial t} = -\frac{\partial p}{\partial x} + \frac{\partial \tau}{\partial z} \qquad (6)$$

Outside the boundary layer, the velocity is given by the free stream velocity u_0 and the shear stress becomes $\tau = 0$. A simple integral approach is applied to solve the momentum equation

$$\tau_w = \int_{z_0}^{\delta+z_0} \rho \frac{\partial (u_0 - u)}{\partial t}\, dz = -\int_{z_0}^{\delta+z_0} \frac{\partial \tau}{\partial z}\, dz \qquad (7)$$

Where τ_w is the wall shear stress (WSS) and z_0 is the zero level of the velocity. To solve this boundary layer momentum equation, the shape of the velocity profile is assumed to be logarithmic. This method requires to solve numerically an ordinary differential equation (ODE) (Fredsoe and Deigaard, 1992). Figure (5) shows WSS obtained from Eq. (7) over a half-period for a sinusoidal wave for different values of a_m/k_s.

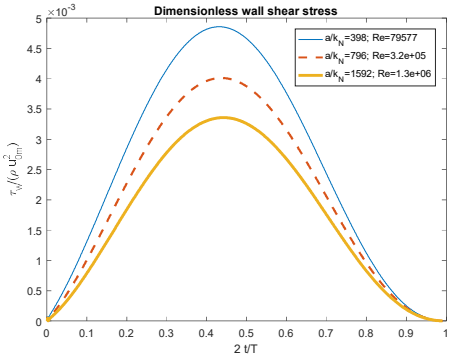

Figure 5. WSS for a sinusoidal wave.

3. Pulsatile flows in arteries

Physiological and cardiovascular fluid mechanics provided an understanding of advanced concepts in fluid mechanics. The study of blood flow in the cardiovascular system is more complicate since blood is a non-Newtonian fluid and arteries are elastic/compliant tubes.

Blood is a two-phase suspension of suspended elements (i.e., red blood cells, white blood cells, platelets) in an aqueous solution. Blood behaves as a non-Newtonian fluid (i.e., the apparent viscosity of blood depends on the shear forces). The most common non-Newtonian models used for the blood are the power law, Casson, and Carreau-Yasuda models (Shibeshi and Collins, 2005). However, in some cases it is assumed as Newtonian. The description of the flow behavior in arterial vessels (elastic tubes) needs three independent variables namely the pressure $p(x,t)$, the fluid velocity $u(x,t)$ (or equivalently the flow rate $Q(x,t)$) and the cross-sectional area $A(x,t)$. The main governing equations are the conservation of mass, momentum (i.e. continuity and momentum equations) and energy conservation which is related to the interaction between the fluid and the tube wall (Morris *et al.*, 2016).

Adequate methods are needed for the quantification of parameters which cannot be obtained experimentally as WSS. WSS is related to several endothelial dysfunction and cardiovascular disease as atherosclerosis (Moore *et al.*, 1994). In elastic tubes, fluid-structure interaction has a considerable effect on the WSS calculations. Computational fluid structure interaction (FSI) simulations allow to quantify time- and space-evolution of wall shear stress (WSS). The oscillatory shear index (OSI) is used to describe the unsteady nature of blood flow in arteries, it is defined as

$$\mathrm{OSI} = \frac{1}{2}\left[1 - \frac{\left|\int_0^T \bar{\tau}_w dt\right|}{\int_0^T |\bar{\tau}_w| dt}\right] \qquad (8)$$

OSI varies between 0 and 0.5. It considers the oscillations in the flow direction: the larger the index, the more important

the wall shear oscillations. Comparisons between time-dependent WSS in rigid and compliant vessels show that rigid wall simulations generally overestimate WSS (Kim *et al.*, 2008).

Adequate quantification of pressure changes during the systolic and diastolic phases of the cardiac cycle is important for accurate prediction of WSS.

The Windkessel model, which is based on an electrical analogy, provides time-dependent pressure during the systolic and diastolic phases (Frank, 1899; Guan, 2016). In the 2-Element Windkessel Model, the resistance of the arterial system and arterial compliance are represented respectively by a resistor and a capacitor (fig. 6.a). In the 4-Element Windkessel Model, in addition to an added resistor which account for this resistance to blood flow due to the aortic valve, an inductor is included to account for the inertia of blood flow in the hydrodynamic model (fig. 6.b).

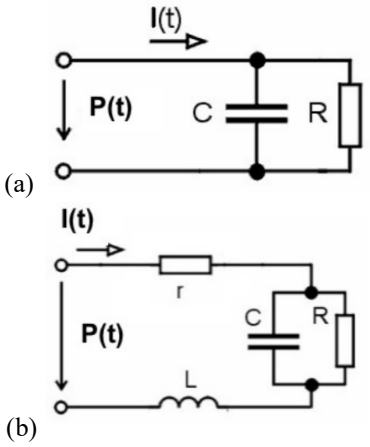

Figure 6. Blood flow in arteries. electric analogy of Windkessel models. (a) 2-Element model, (b) 4-Element model with fluid inertia represented by the inductor L

The Windkessel model is validated by experimental data. Blood flow information was acquired using a cardiac-gated, 2D, respiratory compensated, phase-contrast (PC) cine sequence with through-plane velocity encoding (Karmonik *et al.*, 2014). The cardiac output of the patient was 3.71 L/min, the heart rate 47 beats per minute (cardiac cycle T = 1.277 sec). Figure (7) shows measured and reconstructed time-dependent flow rate Q_t at the level of the ascending aorta. A 15-term Fourier reconstruction of the flow waveforms is given by (Karmonik *et al.*, 2014)

$$Q_t = \text{real}\left\{\sum_{n=0}^{14} Q_n e^{i\omega n t}\right\} \tag{9}$$

where Q_n is the Fourier mode and i is the imaginary unit.

Figure (8) shows time-dependent pressure during the systolic and diastolic phases obtained from the Windkessel model. The dashed line represents the result of the 2-Element Windkessel Model while the solid line is the result of the 4-Element Windkessel Model which allows an accurate description of the measured values (symbols). This is because the 4- Element Windkessel Model accounts all effects: resistances/resistors, arterial compliance/capacitor and especially inertia of blood flow/inductor.

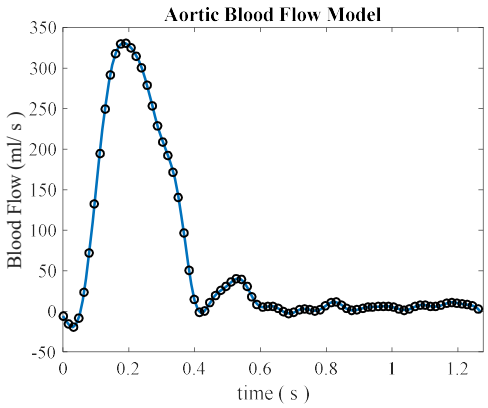

Figure 7. Pulsatile blood flow. Ascending aortic flow waveforms (in ml/sec) measured by the (PC)-MRI sequence (Karmonik *et al.*, 2014).

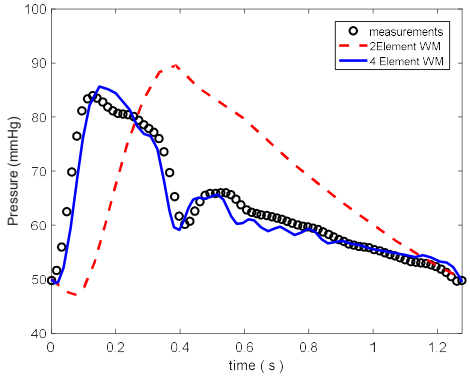

Figure 8. Pressure. Dashed-line: 2-Element model; Green solid line: 4-Element model (with inertia: inductance L)

It is possible to describe the deformation of the vessel walls (variation in the cross-sectional area or diameter) due to a variation in the transmural (internal minus external) pressure p_{tm}, by a pressure-area $p - A$ constitutive relation given by (Absi 2018)

$$\frac{p_{tm}}{\beta_1} = C_v\left(1 - \sqrt{\frac{A_0}{A}}\right) \tag{10}$$

Where $C_v = 1$ if $v = 0$ and $C_v = (1/(1-v^2))\sqrt{A_0/A}$ if $v \neq 0$. where $\beta_1 = E\, h_0/R_0$, E is the Young's modulus, R_0 and, v the Poisson's ratio, h_0 are respectively the internal radius and the thickness at p_{tm}=0. The arterial capacitance per unit length or cross-sectional compliance C_c may be calculated assuming that vessel length does not vary with transmural pressure.

$$C_c = \frac{dA}{dp} \tag{11}$$

4. Pulsed flows for cleaning of industrial equipment

The formation of fouling deposits in process plants of food, cosmetic and pharmaceutical industries is of crucial importance since it can affect microbial sterility and alter the purity of the product. In practice, cleaning is expensive, not only through the cost of the cleaning process by itself, but also by the cost of lost production and the environmental costs related to waste treatment. The actual situation is such cleaning in place (CIP) protocols need to be more optimal particularly by reducing excess energy. The optimization needs an adequate quantification of the required forces/energy required for deposits removal. However, these forces are affected by the interaction between deposits and surfaces. The main questions about the process of deposit removal are as follows: How cleaning is affected by process variables? How to initiate fracture in deposits?

Cleaning is a complex phenomenon. Research conducted during the last decades allowed to highlight the effect of hydrodynamic of the cleaning fluid on CIP efficiency (Grasshoff, 1992). Particularly the importance of the flow parameters such as fluid velocity (Schlussler, 1976), shear forces at fluid/equipment interfaces or WSS (Sharma *et al.*, 1991). The mean WSS was related to the removal of clay deposits and bio-film (Bergman and Tragardh, 1990, Hall 1998). In industrial CIP procedures, the used flow for cleaning is in general in turbulent regime (Bénézech and Lalande, 1999).

It is possible to generated flow pulses by bellows units or piston devices allowing low frequencies (<= 2 Hz) (Gillham, 2000) or pulsation generator systems which allows pulsations of high amplitudes and maximum frequency up to 2.86 Hz (Blel *et al.*, 2009). Pulsations conditions were defined by opening-closing times and minimum–maximum flow rate. Instantaneous variations of the velocity is represented by a free stream velocity given by

$$u_0(t) = u_s + u_p \sin(2\pi f t) = u_s(1 + A\sin(2\pi f t)) \quad (14)$$

where f is the frequency of the pulsations (Hz), u_s the steady component, u_p the pulsatile component and $A = u_p/u_s$ the dimensionless amplitude of the pulsations.

The experiments of Lelièvre *et al.* (2002) showed that cleaning depends on both mean WSS and fluctuation rate. Low WSS zones with a high level of turbulence (high fluctuation rate) was shown as very cleanable. Local WSS values were obtained experimentally by using an electrochemical technique. First, the instantaneous value of the wall shear rate $S(t)$ (at the surface of the electrode) is calculated from the instantaneous limiting current, $I(t)$ which is related to the Sherwood number (Reiss and Hanratty, 1963; Sobolik *et al.*, 1987). The instantaneous value of the wall shear rate $S(t)$ is written as the sum of mean and fluctuating values as

$$S(t) = \bar{S} + s(t) \text{ with } \overline{s(t)} = 0 \quad (12)$$

The fluctuations were quantified by the fluctuating rate FR defined by

$$FR = \frac{\sqrt{\overline{s^2}}}{\bar{S}} \quad (13)$$

The mean WSS is obtained by multiplying the mean wall shear rate $\bar{S}$ by the fluid viscosity.

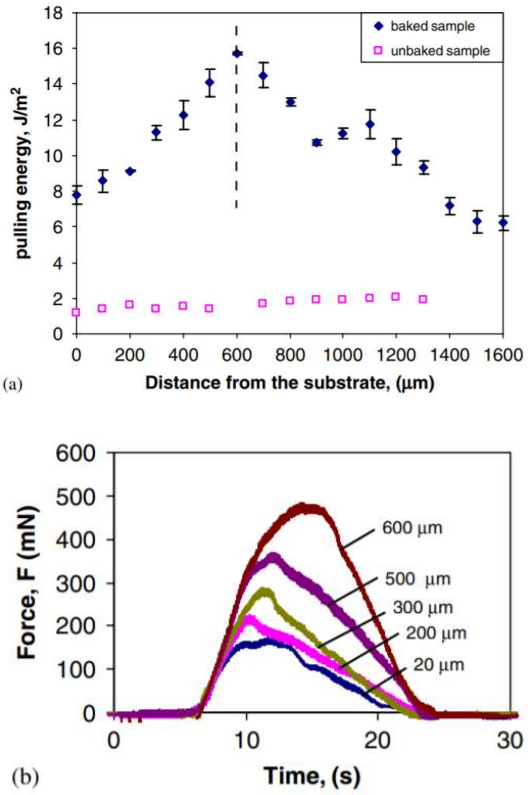

Figure 9. (a) Pulling energy required to disrupt baked and unbaked tomato deposits, as a function of probe cut height above the surface, (b) force–time behavior of baked tomato deposits as a function of probe height above the surface (Liu *et al.*, 2006).

We investigate the efficiency of WSS generated by pulsed flows in removal of tomato deposits (Liu *et al.*, 2006), Figure (9) shows pulling energy/force corresponding to a range of different heights above a surface, from 20 to 1500 μm for baked and unbaked tomato deposits obtained by Liu *et al.* (2006). For the unbaked data, the energy per unit surface (E/S) required to scrape the deposit is about $1\,\mathrm{J/m^2}$ and $2\,\mathrm{J/m^2}$ (Fig. 9.a). The baked data show that the pulling energy increases with height from the surface, up to $16\,\mathrm{J/m^2}$ then it decreases with distance from the surface until $6\,\mathrm{J/m^2}$ (Fig. 9.a). From the relation between WSS and head loss, it is possible to write a relation between the energy per unit surface (E/S) in J/m² and the WSS as

$$\tau_w = \frac{E}{S\,L} \quad (15)$$

Where L and S are respectively the length and surface of a pipe. For a pipe length of 1 meter, the WSS is therefore equal to the pulling energy (energy per unit surface). Eq. (15) is used to obtain experimental values of WSS from measured data of pulling energy (fig. 9.a). For the unbaked data, the required WSS to scrape the deposit is about 1-2 Pa and for the baked data it is between 6 and 16 Pa. Figure (9.b) shows that the behavior of the time-dependent force (for 600 μm) is similar to the shape of the WSS of the first half-period (Fig. 5). The shape of the time-dependent force (Fig. 9.b, amplitude, initial and final times about $7s$ and $23s$, …), could provide indications about the parameters of the used pulsed flow.

For a given pulsed flow, it is possible to calculate mean WSS values from computational fluid dynamics (CFD) simulations based on the Reynolds-averaged Navier-Stokes (RANS) equations or by simple tools as the momentum integral method. In the present simulations, we use Eq. (7) to calculate WSS. To be efficient for the removal of tomato deposits, the flow WSS should be at least equal to the required values of WSS obtained from Eq. (15) and fig (9.a).

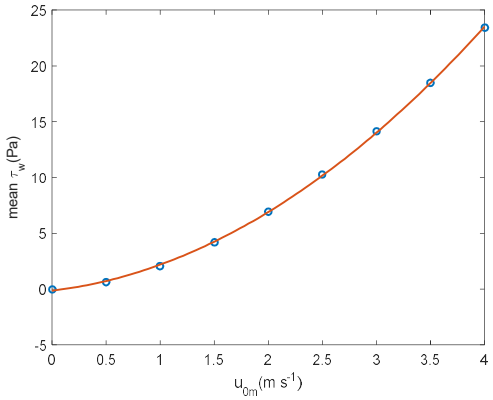

Figure 10. Mean WSS for different free stream velocity values for a period T=2s

Figure (10) presents mean WSS for different free stream velocity values. It shows that velocities about 0.5 and $1m/s$ allow removal of unbaked tomato ($\tau_w \approx$ 2Pa, fig. 9.a) while larger values up to $3m/s$ are needed for the cleaning of baked one ($\tau_w \approx$ 16Pa, fig. 9.a). However, large values of velocities require excess energy. An optimization study requires the use of low velocities and an adequate period/frequency which will allow removal of deposits with low energy. We use the lowest value of velocity namely $0.5m/s$ to investigate the effect of period/frequency on deposit removal. WSS values (Fig. 11) show that a high frequency >3Hz is needed to clean the unbaked tomato. These frequencies seem hardly obtainable by pulsation generator systems (maximum frequency up to 2.86 Hz, Blel *et al.*, 2009) and therefore it seems not possible to clean baked tomato at this velocity and frequencies. The optimization study needs more simulations in order to find the more optimal velocity/frequency values allowing cleaning at low costs.

Figure (12) shows that for the same velocity of 0.5m/s the maximum WSS is about 1.8 Pa and therefore could be able to remove the unbaked tomato deposits. The main question is about the use of mean or maximum WSS. Literature review showed that most studies use the mean WSS. However, for these pulsed flows, the pick WSS plays a particular role. More investigations are needed to know how it will be considered in cleaning of industrial equipment.

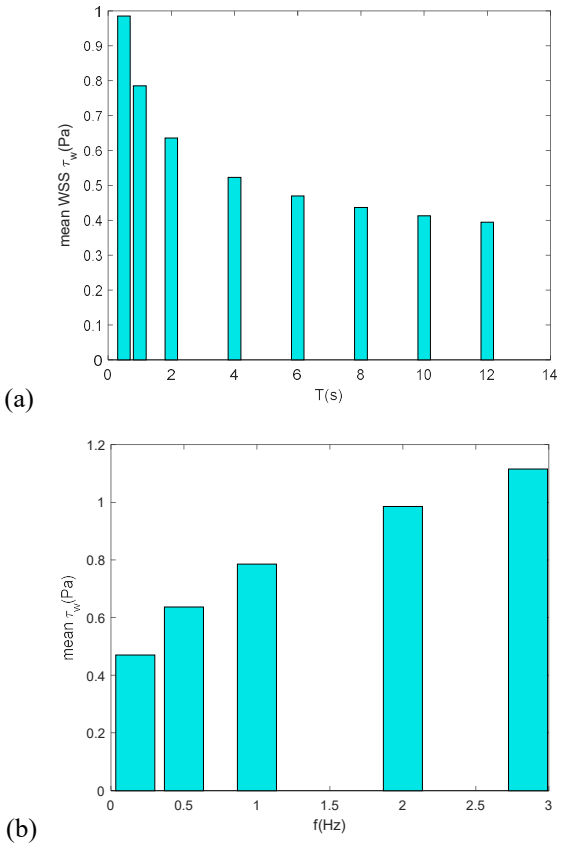

Figure 11. Mean WSS for a free stream velocity of $u_{0m} = 0.5m/s$. (a) for different periods, (b) for different frequencies

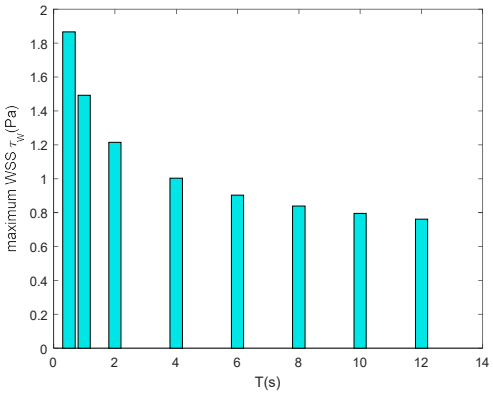

Figure 12. Maximum WSS vs period for free stream velocity of $u_{0m} = 0.5m/s$.

5. Conclusions

The research in fluid mechanics related to periodic (oscillatory and pulsatile) flows is of high interest due to the potential applications in the environmental/coastal, biological/health/Medical and bio-industrial/chemical sectors. Marine and coastal environment is dominated by waves/oscillatory flows. In the circulatory system, the blood flow is pulsatile. In bio-industries, pulsed flows are used in cleaning of fouling deposits. Wall shear stress (WSS) is a parameter of common interest. In coastal engineering, it is involved in incipient motion of sediments and turbulence modeling. In medicine, WSS is related to several endothelial dysfunction and cardiovascular disease as atherosclerosis. In industry, deposit removal depends on WSS values.

In coastal engineering both RANS turbulence models and analytical formulations are used. Analytical models need WSS which can be obtained simply by the momentum integral method. In cardiovascular systems, calculations of WSS is more complicated since blood behaves as a non-Newtonian fluid and arteries are compliant tubes. In elastic tubes, fluid-structure interaction has a considerable effect on the WSS calculations. Oscillatory shear index (OSI) is used to quantify the effect of the vessel wall compliance. The Windkessel model, which is based on an electrical analogy, provides accurate time-dependent pressure during the systolic and diastolic phases. The 4-Element Windkessel Model considers the resistance of the arterial system and the aortic valve by two resistors. The arterial compliance is taken into account by a capacitor and the inertia to blood flow by an inductor. In CIP, the fluctuating rate FR needs to be considered. We investigated the efficiency of WSS generated by pulsed flows in the removal of tomato deposits. Large values of velocities require excess energy. WSS was calculated by the momentum integral method. Results show that for the optimization study, it is more interesting to use a flow with a low velocity and find the adequate period/frequency value. It could be interesting to investigate the effect of flow reversal associated to an oscillatory flow which could be more efficient.

Our study shows that these different flows require deep understanding of advanced concepts in fluid mechanics to allow an adequate quantification of the involved parameters. It is important to share and use knowledge beyond disciplines especially in fluid mechanics which is at the crossroads of different applications. This study aims transdisciplinary research strategies toward a holistic approach.

Acknowledgments

The first part of this work was undertaken during the visit of the author at Tohoku University. The author is grateful for the financial support provided by Japan Society for the Promotion of Science (JSPS), within the FY2010 JSPS Invitation Fellowship Program for Research in Japan (No. S-10168).

References

Absi, R. 2008. Analytical solutions for the modeled k-equation, *ASME J. Appl. Mech,* 75(4), 044501

Absi, R. 2010. Concentration profiles for fine and coarse sediments suspended by waves over ripples: An analytical study with the 1-DV gradient diffusion model, *Advances in Water Resources*, 33, 411-418.

Absi R. 2018. Revisiting the pressure-area relation for the flow in elastic tubes: application to arterial vessels, *Series on Biomechanics*, 32(1), 47-59.

Absi R., Tanaka H., Kerlidou L. and André A. 2012. Eddy viscosity profiles for wave boundary layers: validation and calibration by a k-ω model, *Proc. 33th International Conference on Coastal Engineering,* Santander, Spain, ASCE.

Bénézech, T. and Lalande, M. (1999). Le Nettoyage en Place (NEP). In J. Y. Leveau, & M. Bouix (Eds.), Nettoyage, desinfection et Hygiene dans les bio-industries (pp. 341–364). France: Coll Sciences et techniques agroalimentaires, Tec & Doc.

Bergman, B. O. and TrHagardh, C. (1990). An approach to study and model the hydrodynamic cleaning effect. *Journal of Food Process Engineering*, 13, 135–154.

Blel, W., Le Gentil-Lelièvre, C., Bénézech, T., Legrand, J. and Legentilhomme, P. (2009) Application of turbulent pulsating flows to the bacterial removal during a cleaning in place procedure. Part 1: Experimental analysis of wall shear stress in a cylindrical pipe, *Journal of Food Engineering*, 90, 422–432.

Canic, S., 2002. Blood flow through compliant vessels after endovascular repair: wall deformations induced by the discontinuous wall properties. *Computing and Visualization in Science*, 4(3),147-155.

Frank, O. 1899. The basic shape of the arterial pulse. First treatise: Mathematical analysis Translation of Otto frank's paper “Die Grundform des arteriellen Pulses”, *Zeitschrift Für Biologie*, 37, 483–526.

Fredsoe, J., and R. Deigaard. 1992. *Mechanics of coastal sediment transport*, World Scientific Publishing, 369 pp.

Gillham, C.R., Fryer, P.J., Hasting, A.P.M., and Wilson, D.I., 2000. Enhanced cleaning of whey protein soils using pulsed flows. *Journal of Food Engineering*, 46, 199–209.

Grasshoff, A. 1992. Hygienic design: The basis for computer controlled automation. Food and Bioproducts Processing, *Transactions of The Institution of Chemical Engineers* Part C, 70, 69–77.

Guan, D., Liang, F. and Gremaud, P. A. 2016. Comparison of the Windkessel model and structured-tree model applied to prescribe outflow boundary conditions for a

one-dimensional arterial tree model, *Journal of Biomechanics*, 49(9), 1583-1592.

Hall, J. E. (1998). Computational fluid dynamics: A tool for hygienic design. In D. I. Wilson, P. J. Fryer, A. P. M. Hasting (Eds.), Fouling and cleaning in food processing '98 (pp. 144 –151). Cambridge: Jesus College.

Hsu, T.-W. and C.-D. Jan. 1998. Calibration of Businger-Arya type of eddy viscosity model's parameters. *Journal of Waterway, Port, Coastal and Ocean Engineering*, ASCE, Vol. 124(5), 281-284.

Jensen, B. L., Sumer, B.M. and Fredsoe, J. 1989. "Turbulent oscillatory boundary layers at high Reynolds numbers", *Journal of Fluid Mechanics*, 206, 265-297.

Jonsson, I.G. 1966. Wave boundary layers amd friction factors, *Proc. 10th International Conference on Coastal Engineering*, Tokyo, Japan, ASCE.

Kajiura, K. 1968. A model of the bottom boundary layer in water waves. *Bulletin of the Earthquake Research Institute*, 46, 75-123.

Karmonik C., Brown A., Debus K., Bismuth J. and Lumsden A.B. (2014) CFD Challenge: Predicting Patient-Specific Hemodynamics at Rest and Stress through an Aortic Coarctation. STACOM 2013. Lecture Notes in Computer Science, vol 8330. Springer, Berlin, Heidelberg

Kim, Y.H., Kim J.E., Ito, Y., Shih, A.M., Brott B. Anayiotos, A. 2008. Hemodynamic analysis of a compliant femoral artery bifurcation model using a fluid structure interaction framework. *Ann Biomed Eng.*, 36(11). 1753-63.

Lelièvre, C., Legentilhomme, P., Gaucher, C., Legrand, J., Faille, F. and Bénézech, T., 2002. Cleaning in place: effect of local wall shear stress variation on bacterial removal from stainless steel equipment. *Chemical Engineering Science*, 57, 1287–1297.

Liu, H. and Sato. S. 2006. A two-phase flow model for asymmetric sheet-flow conditions. *Coastal Engineering*, 53, 825-843.

Liu, W., Zhang, Z. and Fryer, P. J. (2006). Identification and modelling of different removal modes in the cleaning of a model food deposit. *Chemical Engineering Science*, pp. 7528-7534.

Nielsen, P. 1992. *Coastal bottom boundary layers and sediment transport*, World Scientific, 324 p.

Menter, F.R. 1994. Two-equation eddy-viscosity turbulence models for engineering applications. *AIAA Journal*, 32 (8), 1598-1605.

Moore Jr. J.E., Xu, C., Glagov, S., Zarins, C.K. and Ku, D.N. 1994. Fluid wall shear stress measurements in a model of the human abdominal aorta: oscillatory behavior and relationship to atherosclerosis, *Atherosclerosis*, 110, 225-240.

Morris, P.D., Narracott, A., von Tengg-Kobligk, H., Silva Soto, D.A., Hsiao, S., Lungu, A., Evans, P., Bressloff, N.W., Lawford, P.V., Hose, D.R. and Gunn, J.P. 2016. Computational fluid dynamics modelling in cardiovascular medicine. *Heart*, 102:18-28.

Mynard, J.P., Davidson, M.R., Penny, D.J. and Smolich, J.J. 2010. A numerical model of neonatal pulmonary atresia with intact ventricular septum and RV-dependent coronary flow. *Int. J. Numer. Meth. Biomed. Engng.*, 26(7), 843-861.

Myrhaug, D. 1982. On a theoretical model of rough turbulent wave boundary layers, *Ocean Engineering*. 9(6), 547-565.

Rammos, K.S., Koullias, G.J., Papou, T.J., Bakas, A.J., Panagopoulos, P.G. and Tsangaris, S.G. 1998. A computer model for the prediction of left epicardial coronary blood flow in normal, stenotic and bypassed coronary arteries, by single or sequential grafting. *Cardiovascular Surgery*, 6(6), 635-648.

Reiss, L.P. and Hanratty, T.J., 1963. An experimental study of the unsteady nature of the viscous sublayer. *AIChE Journal*, 8, 154–160.

Sharma, M. M., Chamoun, H. and Sita Rama Sarma, D. S. H. 1991. Factors controlling the hydrodynamic detachment of particles from surfaces. *Journal of Colloid interface Science*, 149(1), 121–134.

Schlussler, H. J. 1976. Zur Kinetik von Reinigungsvorg angen an festen Oberflachen. *Brauwissenschaft*, 29, 263–268.

Shibeshi, S.S. and Collins, W.E. 2005. The rheology of blood flow in a branched arterial system. *Appl. Rheol.*, 15(6), 398–405.

Sleath, J.F.A. 1990. Seabed boundary layers, The Sea, Vol. 9: Ocean Engineering Science, Bernard Le Méhauté, Daniel M. Hanes (Eds.), 693-728.

Sobolik, V., Wein, O. and Cermak, J., 1987. Simultaneous measurement of film thickness and wall shear stress in wavy flow of non-Newtonian liquids. *Collection of Czechoslovak Chemical Communications*, 52, 913–928.

Suntoyo, and H. Tanaka. 2009. Effect of bed roughness on turbulent boundary layer and net sediment transport under asymmetric waves, *Coastal Engineering*, 56(9), 960-969.

Tanaka, H. and Thu., A. 1994. Full-range equation of friction coefficient and phase difference in a wave-current boundary layer, *Coastal Engineering*, 22, 237-254.

van Rijn, L.C. 1993. *Principles of sediment transport in River, Estuaries and Coastal Seas*. Aqua Publishing, Amsterdam.